Heliyon 9 (2023) e20183

Contents lists available at ScienceDirect

Heliyon

journal homepage: www.cell.com/heliyon

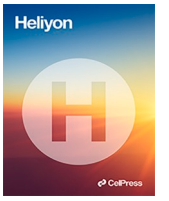

Syndecan-2 modulates the YAP pathway in epithelial-to-mesenchymal transition-related migration, invasion, and drug resistance in colorectal cancer

Yang Yang [a,1], Yong Li Cao [a,1], Wen Hang Wang [b,1], Shou Sen Shi [a], Yuan Yao Zhang [a], Bing Bing Lv [a], Wei Wei Yang [a], Ming Li [a], Dong Wei [a,*]

[a] Institute of Anal Colorectal Surgery, The 989th Hospital of the Joint Logistics Support Force of PLA, Luoyang, 471031, Henan Province, China
[b] Department of Anorectal, Zhumadian Central Hospital, Zhumadian, 463000, Henan Province, China

ARTICLE INFO

Keywords:
YAP
SDC2
Colorectal cancer
Metastasis
Drug resistance

ABSTRACT

Epithelial-to-mesenchymal transition (EMT) is associated with an invasive phenotype in colorectal cancer (CRC). Here, we examined the roles of YES-associated protein (YAP) and syndecan-2 (SDC2) in EMT-related progression, invasion, metastasis, and drug resistance in CRC. The expression levels of YAP and SDC2 in CRC patient tumor tissue were quantified by PCR and western blotting. EMT-associated characteristics were assessed using Transwell assays and immunohistochemistry. Co-immunoprecipitation, glutathione S-transferase pull-down, and luciferase reporter assays were used to assess interactions between YAP and SDC2. YAP was found to be highly expressed in tumor tissue from 13/16 CRC patients, while SDC2 was highly expressed in the tumor tissue of 12/16 CRC patients. Overexpression of YAP in colon cancer cells led to increased cell viability, invasion, migration, and oxaliplatin resistance demonstrating that YAP plays a role in EMT. In addition, overexpression of YAP led to decreased expression of the large tumor suppressor kinase 1 (LATS1) and mammalian sterile 20-like kinases (MST1/2). Decreased LATS1 expression was associated with increased levels of cell proliferation. Knockdown of YAP by shRNA interference led to decreased cell invasion, migration, and drug resistance in colon cancer cells and reduced tumorigenesis in a mouse xenograft model. Finally, we established that YAP interacted with SDC2, and demonstrated that SDC2 mediated the YAP pathway through the EMT-related factors BMP4, CTGF and FOXM1.

1. Background

The incidence of colorectal cancer (CRC), a major malignant disease, is increasing in low to middle-income countries [1,2]. The epigenetic and genetic alterations associated with CRC include methylation, loss of genetic integrity, chromosomal instability related to the activation of proto-oncogenes and inactivation of tumor suppressor genes, and microsatellite instability [3]. CRC is derived from rapidly dividing intestinal stem cells that have an increased susceptibility to mutation [4]. Approximately 20% of patients with CRC go on to develop metastasis, especially in the lungs and liver. At present, the latent cancer stem cells that become metastatic tumors are

* Corresponding author.
E-mail address: wd150yyw5k@yeah.net (D. Wei).
[1] contributed equally.

https://doi.org/10.1016/j.heliyon.2023.e20183
Received 2 April 2023; Received in revised form 7 September 2023; Accepted 13 September 2023
Available online 21 September 2023

unresponsive to therapy [5].

Epithelial-to-mesenchymal transition (EMT), the process by which epithelial cells acquire mesenchymal phenotypes, promotes tumor progression, invasion, and metastasis and is modulated by a number of pathways including transforming growth factor-beta (TGF-β) and WNT/β-catenin pathways [6,7]. During cancer progression, the wound healing process results in the infiltration of immune cells, which is associated with EMT [8]. The upregulation of EMT during chronic illnesses such as cancer results in fibrosis and contributes to metastasis [9]. The upregulation of EMT-promoting factors in CRC is associated with a more invasive phenotype whereby cells with polarized epithelial characteristics transform into a migratory mesenchymal phenotype [10]. The mesenchymal phenotype is associated with reduced levels of E-cadherin and the overexpression of mesenchymal markers such as fibronectin and vimentin [11].

The YES-associated protein (YAP) is involved in the regulation of a number of pathways including the Hippo, TGF-β, PI3K/AKT, p53, and WNT/β-catenin signaling pathways, and has been implicated in the activation of EMT in several cancers [12–14]. The dephosphorylated form of YAP accumulates in the nucleus of rapidly dividing cancer cells where it participates in cell division and tumorigenesis [15]. Detachment of a cell from the extracellular matrix leads to the upregulation of the large tumor suppressor kinase 1/2 (LATS1/2) and subsequent phosphorylation and inhibition of YAP, which leads to apoptosis under normal conditions [16]. Migrating cancer cells have reduced levels of LATS1/2 and, therefore, elevated levels of YAP. Genes encoding the mammalian sterile 20-like kinases (MST1/2) also negatively regulate YAP by activating LATS kinases through phosphorylation [17].

Syndecan-2 (SDC2) is a transmembrane (type I) heparan sulfate proteoglycan that contains a receptor for ECM proteins and participates in cell-matrix interactions [18]. SDC2 is thought to play a role in metastasis through its association with EMT and has been implicated in several malignancies including CRC [19,20]. Recent studies have shown that aberrant methylation of the SDC2 gene and other genes may contribute to tumorigenesis and act as a potential noninvasive marker in CRC [21,22]. Transcription factors that are known to associate with the SDC2 gene and are involved in cell cycle progression include those activated by bone morphogenetic protein 4 (BMP4) and connective tissue growth factor (CTGF), as well as forkhead box M1 (FOXM1). BMP4 is a member of the TGF-β pathway that regulates the SMAD family of transcription factors by encoding a ligand that binds to TGF-β receptors [23]. CTGF is associated with wound healing and fibrosis and is thought to induce sustained fibrosis through interactions with TGF-β [24]. FOXM1 plays a key role in cell cycle progression and is thought to promote the growth and metastasis of CRC through activation of the β-catenin signaling pathway [25].

In this study, we investigated the molecular mechanisms of SDC2 in relation to YAP and its associated proteins LATS1, MST1, and MST2. We examined the role of YAP in the migration, invasion, and drug resistance of CRC cells by assessing EMT-associated characteristics. Finally, we examined the association between YAP and SDC2, and determined how this interaction affected the EMT-related factors BMP4, CTGF, and FOXM1.

2. Materials and methods

2.1. Ethics statement

Human colon tissue samples were collected from patients after obtaining written informed consent. The study was approved by the Institutional Review Committee of The 989th Hospital of The Joint Logistics Support Force of PLA. The ethical approval number was 989H–20190708011.

2.2. Patient samples

Tumor and paired adjacent normal tissues were collected from colon cancer patients who received treatment at The 989th Hospital of The Joint Logistics Support Force of PLA, immediately sectioned and stored in RNAlater (Ambion, Austin, TX, USA). Samples were then analyzed by quantitative real-time PCR (qRT-PCR), western blotting, and immunohistochemistry. None of the patients had received neoadjuvant therapy. This study was approved by the Ethics Committee of The 989th Hospital of The Joint Logistics Support Force of PLA and in accordance with the ethical standards outlined in the Declaration of Helsinki. All participants gave their written informed consent. Collected samples were used for western blotting, qRT-PCR, and immunohistochemical analyses.

2.3. Cell lines and culture

All cell lines were obtained from the American Type Culture Collection (Manassas, VA, USA), including the human colonic epithelial cell lines (HCoEpiC), colon cancer cell line (HCT116) and CRC cell line (HT29). All cell lines were passaged in our laboratory for less than six months and maintained according to the supplier's instructions. The cell lines were found to be free of mycoplasma infection and their authenticity was verified by DNA fingerprinting before use.

2.4. Quantitative real-time PCR (qRT-PCR)

Total RNA was isolated from samples using a RNeasy Mini Kit according to the manufacturer's instructions (Qiagen, Hilden, Germany). RNA was reverse transcribed using a Reverse Transcription Kit (Applied Biosystems, Foster City, CA, USA) and qPCR was performed on the cDNA using SYBR green reagent (Applied Biosystems) and gene-specific primers. Endogenous β-actin was used to normalize the data. The following PCR conditions were used: 40 cycles of denaturation at 95 °C for 30 s, annealing at 60 °C for 30 s and

elongation at 72 °C for 120 s. The following primers were used: YAP, forward: 5′-TGACCCTCGTTTTGCCATGA-3′, reverse: 5′-GTTGCTGCTGGTTGGAGTTG-3'; SDC2, forward: 5′-AAACGGACAGAAGTCCTAGC-3′, reverse: 5′-GATAAGCAGCACTGGATGGT-3′; and β-actin, forward: 5′-GTCATTCCAAATATGAGATGCGT-3′, reverse: 5′- GCTATCACCTCCCCTGTGTG-3′.

2.5. Transwell chamber assays

Transwell assays were used to assess the invasive and migratory characteristics of transfected cells. For invasion assays, 1×10^5 cells in serum-free media were seeded into the Matrigel-coated Transwell upper chamber (BD Biosciences, San Jose, CA, USA), while medium containing 10% FBS was placed in the lower chamber. The cells were incubated for 24 h and cells invading the lower chamber were stained with 0.1% crystal violet and photographed. For migration assays, 5×10^4 cells in serum-free media were placed in the upper chamber without Matrigel, while medium containing 10% FBS was placed in the lower chamber. The cells were incubated for 16 h. Then, the average number of cells that had migrated to the lower chamber was determined in five fields.

2.6. Colony formation assay

The ability of cells to proliferate was assessed using the colony formation assay. Briefly, 500 cells were seeded into culture dishes and incubated at 37 °C in 5% CO_2 for 14 days. Cells were fixed in paraformaldehyde and stained with Giemsa solution. The number of colonies were counted and the plates were photographed. In addition, cells were resuspended in 0.3% soft agar in medium containing 10% FBS. After 14 days incubation, cells were stained with 0.005% crystal violet and photographed. The average number of colonies from five separate fields was determined.

2.7. CCK-8 assay

Cell viability was measured using a Cell Counting Kit-8 (Dojindo Laboratories, Kumamoto, Japan). Cells were seeded into 96-well plates at a density of 1×10^4/well. After the indicated treatments, CCK-8 solution was added to the medium at a dilution of 1:10 and cells were incubated at 37 °C for 4 h. Absorbance was measured at 450 nm using a microplate reader (Bio-Rad, Sunnyvale, CA, USA).

2.8. Western blot analysis

Protein was extracted from samples using RIPA buffer and quantified using a BCA Protein Assay Kit (Pierce, Rockford, IL, USA). β-actin was used as an internal loading control. Proteins were separated by polyacrylamide gel electrophoresis and then transferred to polyvinylidene fluoride membranes. Membranes were blocked, then incubated overnight at 4 °C with primary antibodies, followed by incubation with secondary antibodies for 1 h at room temperature the following day. Protein signals were detected on membranes by enhanced chemiluminescence (Millipore, Burlington, MA, USA) and images were captured using a ChemiDoc XRS imaging system. Quantity One image software (Bio-Rad) was used for densitometry analysis.

2.9. Immunofluorescence staining

HT29 cells were fixed in 4% paraformaldehyde in PBS for 20 min, and the endogenous peroxidase activity was quenched with 3% hydrogen peroxide. Samples were permeabilized with 0.3% Triton X-100 in PBS for 15 min on ice, pre-blocked for 60 min with bovine serum albumin at room temperature, then incubated with primary antibodies overnight at 4 °C. Staining was detected with the corresponding fluorescein-conjugated secondary antibodies (Jackson ImmunoResearch, West Grove, PA, USA). Slides were mounted and examined using a confocal microscope (Zeiss Instruments).

2.10. Immunohistochemical staining

Tissue slides were first blocked with goat serum for 15 min at room temperature, then incubated with anti-F4/80 antibody (Santa Cruz Biotechnology, CA, USA) overnight at 4 °C. Following washing with PBS, slides were incubated with horseradish peroxidase -conjugated secondary antibodies at 37 °C for 30 min, followed by chromogenic detection using diaminobenzidine tetrahydrochloride as the substrate. Sections were counterstained with hematoxylin. Stained sections were observed under a light microscope (DP73; Olympus).

2.11. In vivo nude mouse xenograft model

All animal studies were approved by the Institutional Animal Care and Use Committee (IACUC) of The 989th Hospital of The Joint Logistics Support Force of PLA. Standard animal care and laboratory guidelines were carried out according to the IACUC protocol. Four-week-old female BALB/c nude mice were injected subcutaneously with 2×10^6 CT29 cells (10 mice per group) and treated with intratumoral injection (40 μL) of Scr, YAP overexpression (YAP OE), or YAP shRNA (shYAP) vectors. Tumor volumes were calculated by the formula: volume = length × $(\text{width}/2)^2$. Immunohistochemical staining was performed using anti-YAP (ab205270; Abcam, Austin, TX, USA), anti-SDC2 (ab191062; Abcam), and anti-Ki-67 (ab8191; Abcam) antibodies. Mice were housed at a temperature of 21 ± 2 °C and 30–70% humidity with a 12 h light/dark cycle, and free access to food and water. Mice were anesthetized by

intraperitoneal injection of 10% chloral hydrate (300 mg/kg) and no signs of peritonitis, pain or discomfort were observed following the injection. Decreased limb tension and corneal reflex indicated the depth of anesthesia. During the 30 day study period, data were collected at specific time points. Every effort was made to reduce the pain of the animals, as well as the number of animals used. A total of 30 mice were used in this experiment. The health of the mice was monitored at the indicated time points (every three days). The humanitarian end point was complete loss of appetite or inability to eat and drink by oneself within 24 h, or depression due to hypothermia (<37 °C) without anesthesia or sedation. The mice were humanely killed by cervical dislocation after samples had been collected. Complete cardiac arrest and dilated pupils were an indication of death.

2.12. Plasmids, lentivirus production, and stable cell line selection

The YAP overexpression and YAP shRNA constructs were generated using SDCPGMLV-CMV-YAP-EF1-ZsGreen1-T2A-Puro and PGMLV-hU6-YAP-CMV-ZsGreen1-PGK-Puro plasmids (Genomeditech, Shanghai, China), respectively. The SDC2 overexpression and SDC2 shRNA constructs were generated using PGMLV-CMV-SDC2-EF1-ZsGreen1-T2A-Puro and PGMLV-hU6-SDC2-CMV-ZsGreen1-PGK-Puro plasmids, respectively. Lentiviral particles were produced by transfecting the psPAX2 and pMD2. G plasmids into HEK293T cells using Lipofectamine 2000 (Invitrogen, Waltham, MA, USA) according to the manufacturer's protocol. Stable cell lines were obtained by infection with the lentiviral particles followed by puromycin selection. The following shRNA sequences were used: SDC shRNA: 5′-GAAACCACGACGCUGAAUATT-3′; YAP shRNA1: 5′-GGTCAGAGATACTTCTTAAAT-3'; YAP shRNA2: 5′-GGGCCTCTTCCTGATGGATGG-3'; YAP overexpression: 5′-CTGAGCCAACAGTGGTAGTA-3'; and SDC2 overexpression: 5′-GATCCCCTGACGATGACTACG-3'. The transfection efficiency was determined by western blotting.

2.13. Immunoprecipitation

Colon cell lysates were prepared using a lysis buffer containing 50 mM Tris (pH 7.4), 150 mM NaCl, 1% Triton X-100, and 1 mM EDTA. Lysates were incubated with protein A agarose-immobilized antibody for 2 h at 4 °C. Following immunoprecipitation, the immunocomplexes were washed with lysis buffer three times and eluted with 2 × SDS sample buffer.

2.14. GST pull-down assay

For the YAP-GST pull-down assay, the YAP-GST fusion protein was expressed in *E. coli* BL21 cells, purified overnight at 4 °C, then immobilized on the glutathione agarose 4B column. HEK-293T cells transfected with Flag-SDC2 were treated as shown in. Then, the cells were lysed with protease inhibitor in NETN buffer, cultured with sepharose, and fixed with the designated YAP-GST protein at

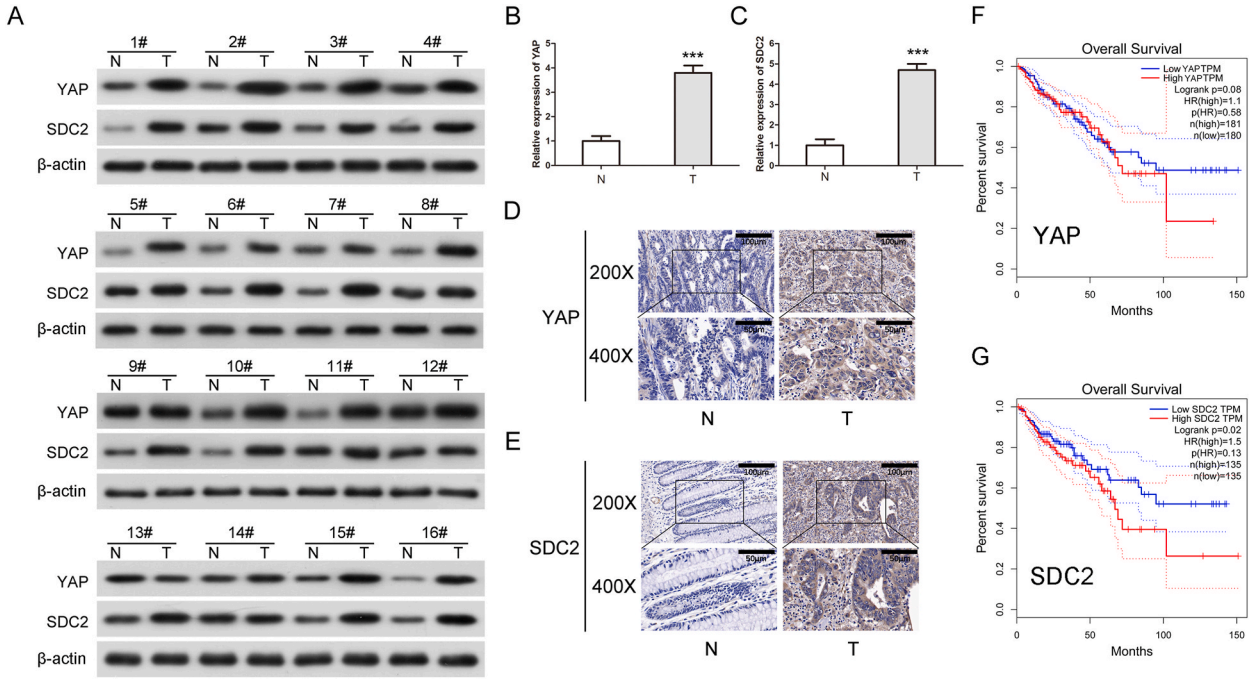

Fig. 1. The expression of YAP and SDC2 in human CRC and normal tissue. (A) Out of 16 CRC patient tissue samples, YAP and SDC2 expression was found in 13 and 12 samples, respectively. (B–C) qRT-PCR was used to assess YAP (B) and SDC2 (C) mRNA expression in human tissues. (D–E) Immunohistochemical analysis of YAP and SDC2 in human tissues. (F-G) The GEPIA database was used to determine the overall survival (OS) of patients based on YAP and SDC2 gene expression levels. ***$p < 0.001$.

4 °C for 8 h. GST beads (Sigma, MO, USA) were used to pull down the YAP/SDC2 complex. Protein bands were detected by Western blot analysis.

2.15. Transient transfection and luciferase assays

Cells were seeded into 12-well plates and transfected with 1 μg of the indicated luciferase vector using Fugene 6. The quantity of

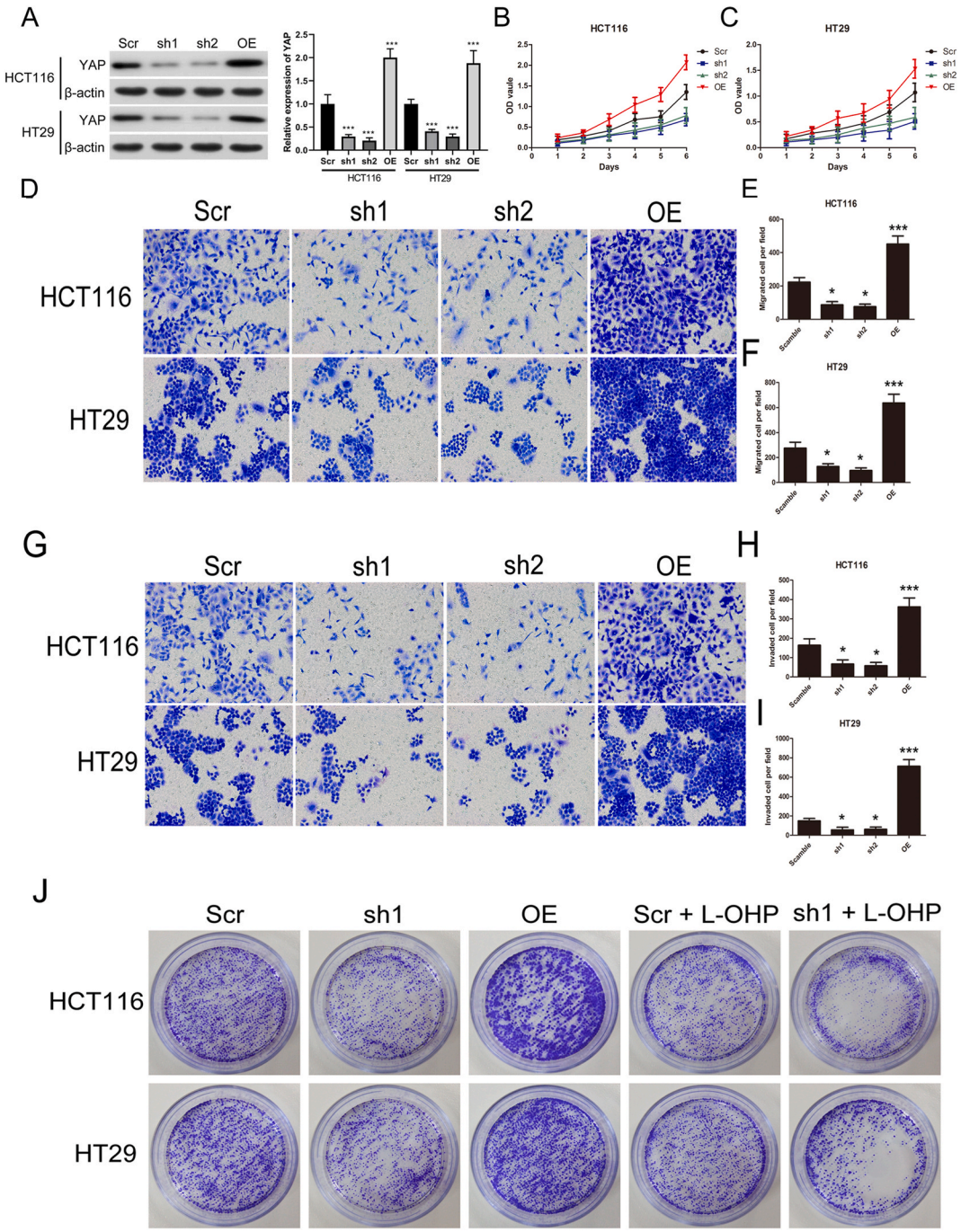

Fig. 2. YAP enhances the cell viability, migration, invasion and drug resistance of HCT116 and HT29 cells. (A) Western blot analysis was used to verify the transfection efficiency of YAP. (B–C) The cell viability of HCT116 (B) and HT29 (C) cells was determined using the CCK-8 assay. (D–F) HCT116 and HT29 cell migration was assessed using the Transwell assay. (G–I) The invasiveness of HCT116 and HT29 cells was measured using the Matrigel Transwell assay. (J) Colony formation assay of HCT116 and HT29 cells. n = 3. *p < 0.05, ***p < 0.001.

total DNA was kept constant. Six hours after transfection, the cells were washed and transduced with the indicated adenovirus. The cells were lysed with Passive Lysis Buffer, and the transcriptional activity was determined using a luciferase assay system (Promega, Madison, WI, USA).

2.16. Statistical analysis

Statistical analysis was conducted using SPSS 18.0 software, and all values are presented as mean ± SEM. Statistical analysis was conducted using a two-tailed Student t-test or one-way analysis of variance, while multiple group comparisons were conducted using one-way analysis of variance and Tukey's post hoc test. A p value of <0.05 is considered statistically significant.

3. Results

3.1. Expression of YAP and SDC2 in human tissue

The Western blot data showing YAP and SDC2 protein expression levels in tissue samples from 16 CRC patients are shown in Fig. 1A. Increased YAP expression was observed in 13 tumor tissue samples, while significantly higher SDC2 expression levels were found in 12 tumor tissues. In addition, qRT-PCR revealed significantly higher YAP and SDC2 mRNA expression levels in CRC tissue (Fig. 1B and C; $p < 0.001$). Immunohistochemical analysis revealed more intense staining of YAP and SDC2 in the CRC tumor tissue than normal tissue (Fig. 1D and E). The GEPIA database was used to determine the overall survival (OS) of patients based on YAP and SDC2 gene expression levels (Fig. 1F and G). High expression of YAP and SDC2 was associated with a significantly decreased OS. Taken together, our results demonstrate that YAP and SDC2 are upregulated in CRC.

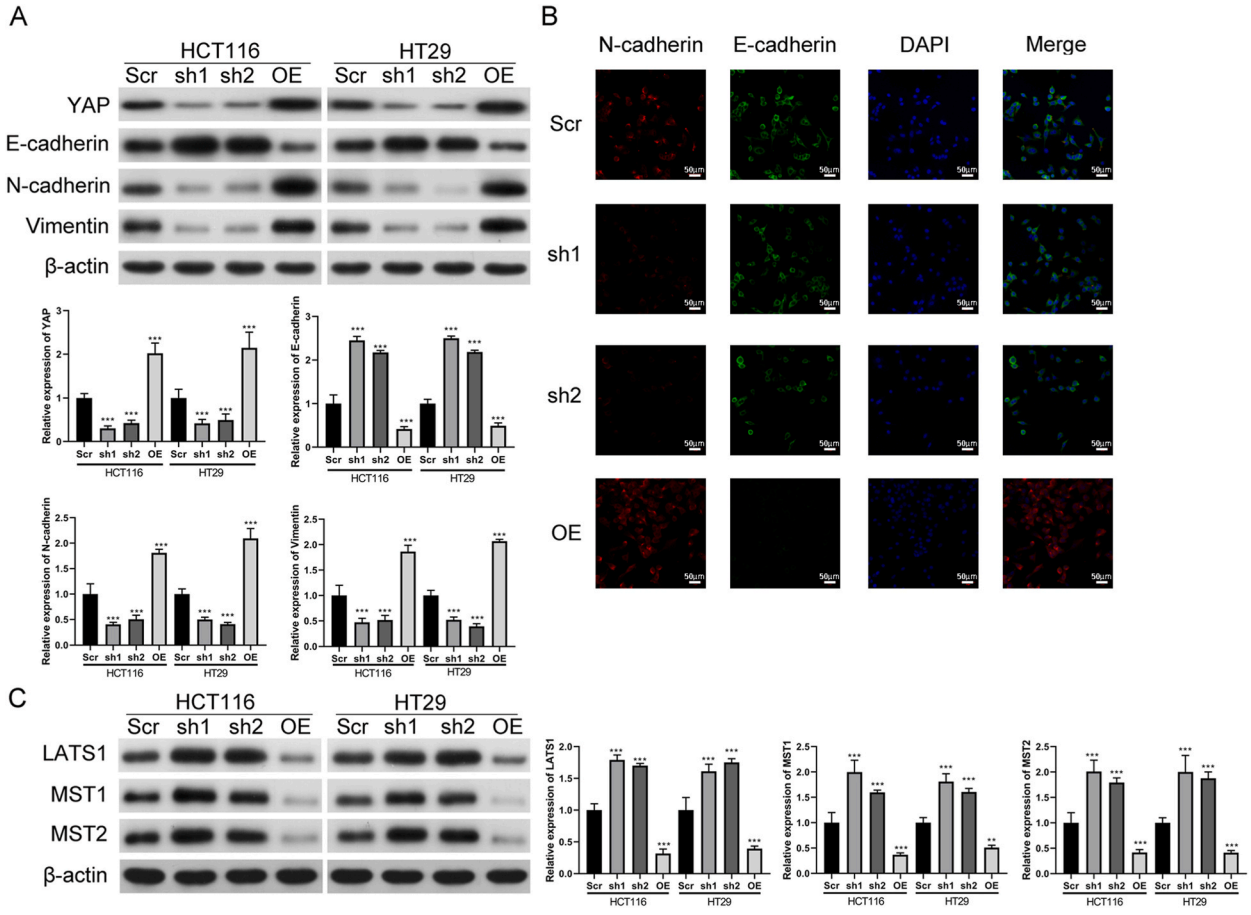

Fig. 3. YAP promotes epithelial-to-mesenchymal transformation (EMT) in colon cancer cell lines. (A) Detection of EMT-related proteins by western blotting. (B) Representative immunofluorescence images showing N-cadherin (red) and E-cadherin (green). (C) Western blot analysis of YAP pathway-related proteins. n = 3. ***$p < 0.001$.

3.2. YAP enhances cell viability, migration, invasion and drug resistance in colon cancer cell lines

To determine the role of YAP in CRC, we transfected the colon cancer cell lines HCT116 and HT29 with either the YAP overexpression vector or YAP shRNA. After confirming the transfection efficiency (Fig. 2A), the effects of YAP overexpression and knockdown on cell viability were determined (Fig. 2B and C). Overexpression of YAP was found to increase the cell viability of both HCT116 and HT29 cells, while knockdown of YAP led to a decrease in cell viability. Overexpression of YAP was also found to significantly increase migration, invasion, and colony formation (Fig. 2D–J), whereas YAP knockdown had the opposite effect. These results demonstrate that YAP promotes proliferation and transformation into a more invasive phenotype in colon cancer cells.

3.3. YAP promotes EMT in colon cancer cell lines

Next, we sought to determine whether YAP drives EMT by examining the expression of EMT-related proteins in cells overexpressing YAP (Fig. 3A and B). A common indicator of ongoing EMT and progression to a metastatic phenotype is the loss of E-cadherin expression and concomitant increase in N-cadherin expression levels. Here, overexpression of YAP led to an increase in N-cadherin and decrease in E-cadherin expression levels, signifying increased EMT. Similarly, overexpression of YAP resulted in increased vimentin expression. In contrast, knockdown of YAP led to an increase in E-cadherin expression with a decrease in N-cadherin expression levels. Next, we examined the effects of YAP overexpression and knockdown on LATS1 and MST1/2, which are associated with the YAP pathway (Fig. 3C). Overexpression of YAP led to downregulation of its upstream factors LATS1 and MST1/2, whereas knockdown of YAP resulted in increased LATS1 and MST1/2 levels. These findings indicate that YAP may be involved in promoting EMT in CRC cells and demonstrate that other components of the YAP pathway may also influence the expression levels of YAP. Specifically,

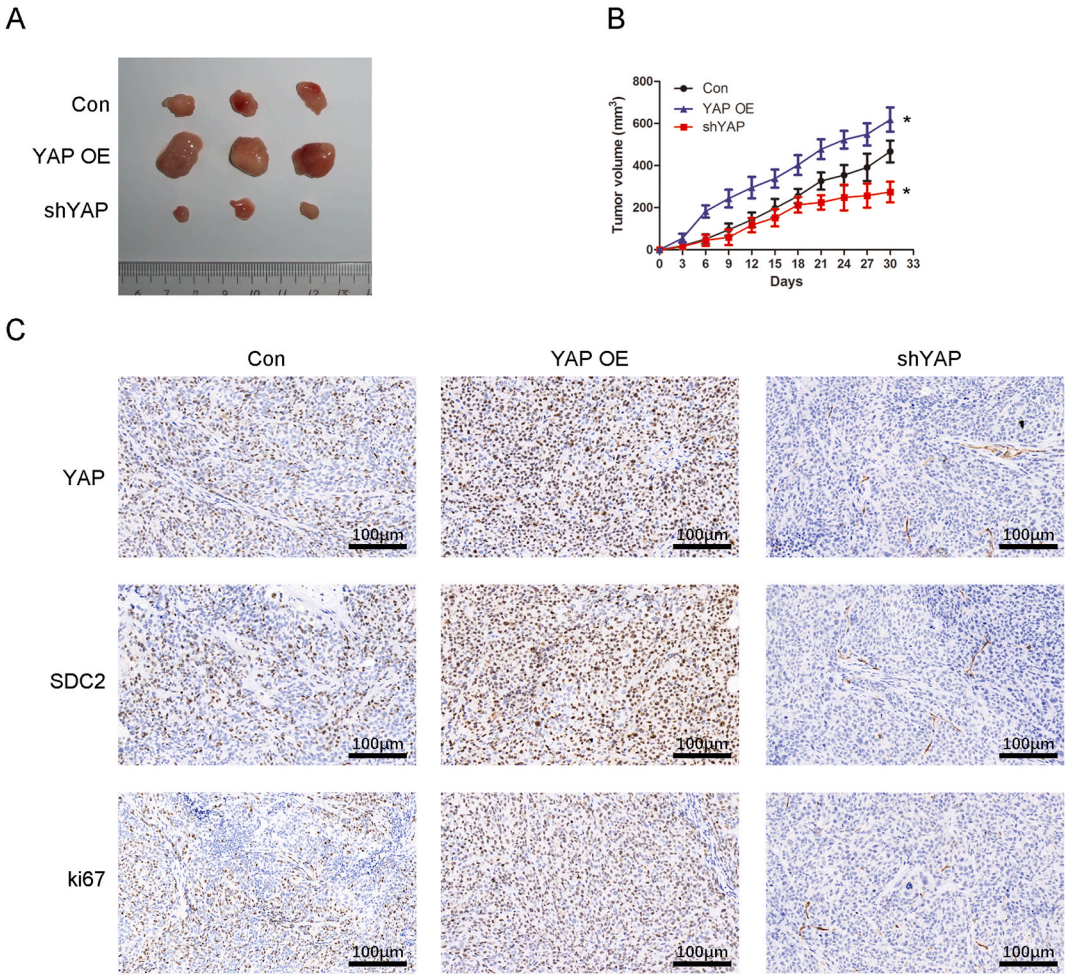

Fig. 4. The effects of YAP knockdown and overexpression in a nude mouse xenograft model. HT29 cells transfected with control (Scr), YAP overexpression (OE), or YAP interference (shYAP) vectors were injected into nude mice to form subcutaneous tumors. (A) Representative images showing the tumors in different treatment groups. (B) Tumor volumes of the different treatment groups. (C) Immunohistochemical analysis of YAP, SDC2, and Ki-67 expression in the subcutaneous tumor tissue from the different treatment groups. $n = 10$. *$p < 0.05$.

downregulation of LATS1 and MST1/2 may increase expression of YAP, thereby activating EMT and promoting a more invasive phenotype.

3.4. The effects of YAP overexpression and knockdown in a nude mouse xenograft model

We constructed a nude mouse xenograft model to examine the effects of YAP overexpression and knockdown on the growth of subcutaneous tumors (Fig. 4A). Knockdown of YAP led to a significant improvement in tumor volume (Fig. 4B), while overexpression of YAP resulted in the largest tumor volume and lowest survival rate. Immunochemical staining revealed that SDC2 and Ki-67, a cell division marker, were upregulated in tumors overexpressing YAP, while silencing YAP expression led to a reduction in SDC2 and Ki-67 levels compared to the control (Fig. 4C). These results provide further evidence that YAP promotes cell division and tumorigenesis.

3.5. EMT, cell invasion, migration, and drug resistance are modulated by YAP through SDC2

To further understand the relationship between YAP and SDC2, we next asked whether overexpression of SDC2 could compensate for knockdown of YAP (Fig. 5A and B). Overexpression of SDC2 in the absence of YAP resulted in increased N-cadherin expression, although not to the same extent as in cells expressing normal levels of YAP, as well as a significant reduction in E-cadherin expression levels. Overall, our findings suggested that YAP has a greater effect on EMT than SDC2. However, overexpression of SDC2 resulted in a significant increase in the migration and invasion of colon cancer cells, even in the absence of YAP (Fig. 5C and D). Similarly, overexpression of SDC2 in the absence of YAP led to increased colony formation and resistance to oxaliplatin (L-OHP) (Fig. 5E). Overall, these results indicate that EMT, cell invasion, migration, and drug resistance are mediated by YAP through SDC2.

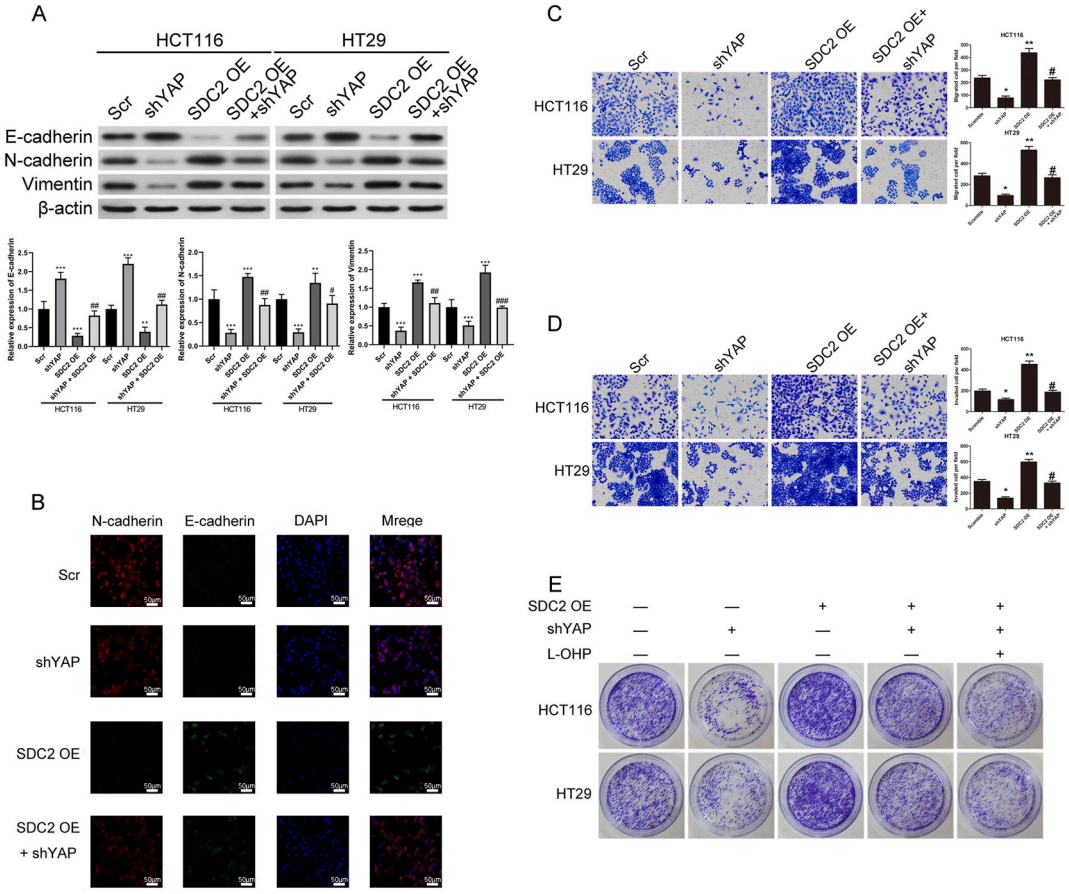

Fig. 5. YAP mediates its effects on epithelial-to-mesenchymal transformation (EMT), cell invasion, migration, and drug resistance through SDC2. (A) Overexpression of SDC2 reverses the effects of YAP knockdown on EMT-related protein expression levels. (B) Representative immunofluorescence images showing N-cadherin (red) and E-cadherin (green) expression in HCT116 and HT29 cells. (C) HCT116 and HT29 cell migration was assessed using the Transwell assay. (D) The invasiveness of HCT116 and HT29 cells was assessed using the Matrigel Transwell assay. (E) Colony formation in HCT116 and HT29. n = 3. *p < 0.05, **p < 0.01 vs Scr, #p < 0.05 vs SDC2 OE.

3.6. Regulation of YAP by transcription factors of SDC2

We next sought to determine whether SDC2-induced transcription factors affected YAP expression. As shown in Fig. 6A, YAP was localized to the nucleus, whereas SDC2 appeared to be localized to the cell membrane when overexpressed. Knockdown of SDC2 resulted in significantly lower YAP expression, while SDC2 overexpression had the opposite effect (Fig. 6B). Similarly, SDC2 knockdown and overexpression led to decreased and increased BMP4, CTGF, and FOXM1 expression levels, respectively (Fig. 6C–E). In addition, knockdown of YAP also decreased BMP4, CTGF, and FOXM1 expression levels in a similar way to SDC2 knockdown. However, overexpression of SDC2 in the absence of YAP significantly increased BMP4, CTGF, and FOXM1 expression levels (Fig. 6F–H). These findings suggest that SDC2 can modulate the expression of YAP, while SDC2-induced transcription factors can also affect YAP expression.

3.7. YAP enhances the transcriptional activity of SDC2

The effects of SDC2 on YAP pathway-related proteins were assessed by western blotting (Fig. 7A). Overexpression of SDC2 led to reduced levels of phosphorylated YAP and increased levels of unphosphorylated YAP, while SDC2 silencing had the opposite effect. Similarly, overexpression of SDC2 in HCT116 cells resulted in lower LATS1, MST1, and MST2 expression levels, while in HT29 cells, MST1 was found to be less affected by SDC2 overexpression. These findings suggested that YAP pathway-related proteins were modulated by SDC2 overexpression. Next, we established that YAP and SDC2 were localized in the nucleus (Fig. 7B). Furthermore, we demonstrated that YAP was immunoprecipitated with a SDC2 antibody in mouse colon epithelial cells (Fig. 7C). Recombinant GST-YAP and myc-SDC2 were used to confirm the direct interaction between YAP and SDC2 (Fig. 7D). In addition, we used a SDC2-luciferase reporter gene assay driven by three canonical SDC2 response elements, LATS1, MST1, and MST2 to show that YAP enhanced the transcriptional activity of SDC2 in a dose-dependent manner (Fig. 7E). Our findings demonstrated that YAP and SDC2 were localized in the nucleus and that endogenous YAP associated with SDC2 in colon epithelial cells to enhance the transcriptional activity of SDC2.

4. Discussion

CRC progression and patient outcome is influenced by the extent of EMT and metastasis [26,27]. Thus, a greater understanding of these processes would further the development of improved therapeutic and management strategies. In this study, we found

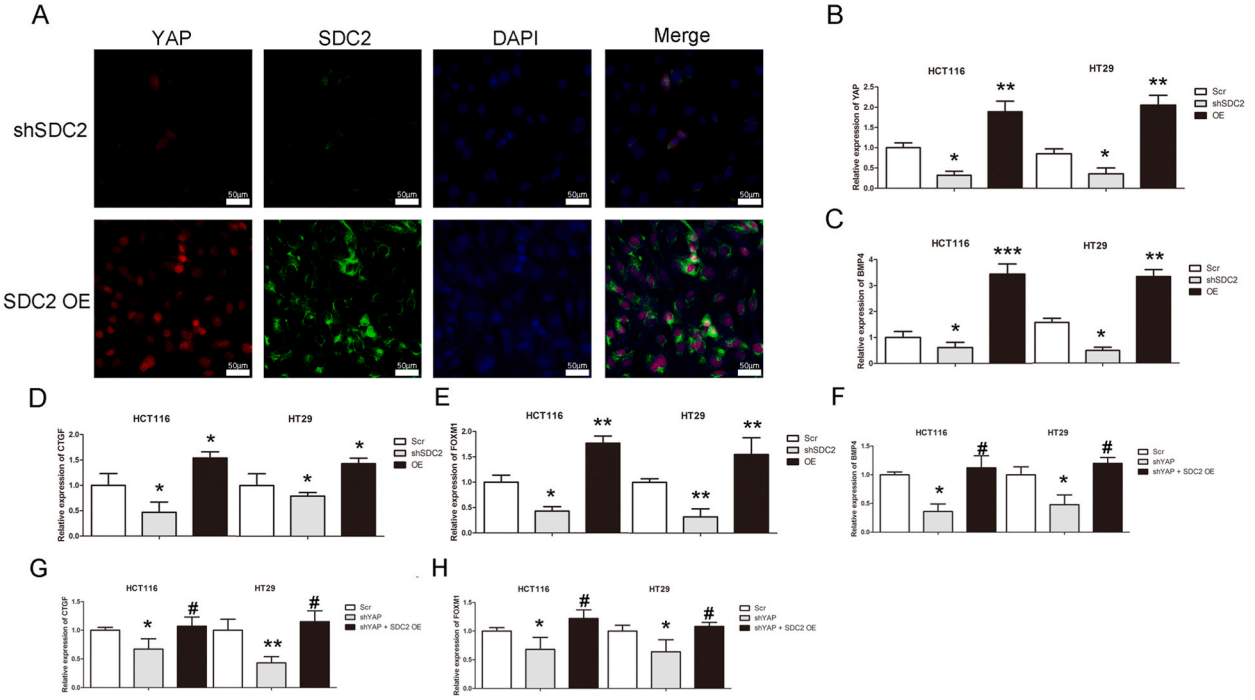

Fig. 6. YAP is regulated by SDC2-induced transcription factors. (A) Representative immunofluorescence images of YAP (red) and SDC2 (green) expression in HCT116 and HT29 cells. (B) qRT-PCR analysis of YAP mRNA levels in HCT116 and HT29 cells. (C–E) qRT-PCR analysis of BMP4 (C), CTGF (D), and FOXM1 (E) mRNA expression levels in SDC2-silenced (shSDC2) and SDC2-overexpressing (SDC2 OE) cells. (F–H) qRT-PCR analysis of BMP4 (F), CTGF (G), and FOXM1 (H) mRNA expression levels in cells transfected with shYAP or shYAP + SDC2 OE. n = 3. *p < 0.05 vs Scr, #p < 0.05 vs shYAP.

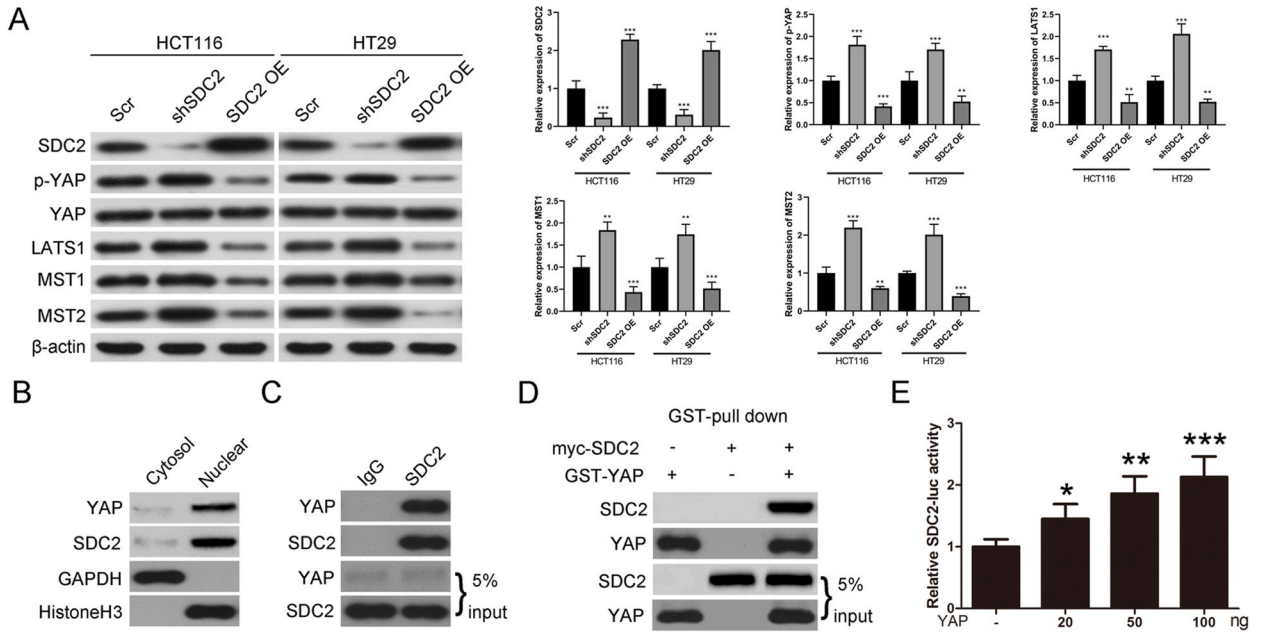

Fig. 7. YAP interacts directly with SDC2 to enhance the transcriptional activity of SDC2. (A) Western blot analysis of p-YAP and YAP pathway-related proteins. (B) YAP and SDC2 are localized in the nucleus. (C) Nude mouse colon epithelial cell lysates were immunoprecipitated with SDC2 antibody or control IgG to examine the interaction between SDC2 and YAP. Representative immunoblots of the input lysate controls (5% of inputs) are also shown. (D) Recombinant GST-YAP and myc-SDC2 were used to examine the direct interaction between YAP and SDC2. (E) Colon epithelial cells were co-transfected with 1 μg SDC2-luc vector and the indicated expression vectors for 48 h, then the luciferase activity was measured. YAP enhances the transcriptional activity of SDC2. n = 3. *p < 0.05, **p < 0.01, ***p < 0.001 vs. empty vector.

upregulation of both YAP and SDC2 in the tumor tissue of CRC patients. Since both YAP and SDC2 are associated with EMT, we next examined their effects on EMT in CRC cells *in vitro* and on tumorigenesis *in vivo*.

First, we examined the effects of YAP and SDC2 on cell viability, invasion, and migration in HCT116 and HT29 cells *in vitro*. We found that cells overexpressing YAP or SDC2 exhibited EMT characteristics, which resulted in a more invasive and drug-resistant phenotype. However, knockdown of YAP ameliorated drug resistance in these cells. Several studies have reported that upregulation of the YAP pathway can promote drug resistance [28–30]. Furthermore, the survival and relapse of CRC patients receiving 5-fluorouracil were worse in tumors expressing high levels of YAP target genes [30]. Silencing or inhibiting YAP or factors associated with the Hippo pathway has previously been shown to increase cell sensitivity to chemotherapeutics [31,32].

In this study, we monitored subcutaneous tumors overexpressing or silencing the expression of YAP in a nude mouse xenograft model. The largest tumor volume and highest cell division rates were found in mice injected with cells overexpressing YAP. Interestingly, we found that SDC2 expression was also upregulated with the overexpression of YAP and downregulated when YAP was silenced, suggesting that YAP may promote cell division and tumorigenesis through SDC2.

YAP is a transcriptional coactivator of the Hippo pathway, which controls a cascade of kinases that regulate cell proliferation and apoptosis [33]. Therefore, we next examined the expression of genes related to the YAP pathway including LATS1, MST1, and MST2. We found that overexpression of YAP led to increased N-cadherin and decreased E-cadherin expression levels, whereas knockdown of YAP had the opposite effect. Furthermore, we found that YAP overexpression resulted in reduced LATS1 and MST1/2 expression levels, whereas YAP silencing led to increased expression levels. Thus, our findings demonstrated that LATS1 and MST1/2 were negatively correlated with YAP expression. Inactivation of LATS1 by promoter methylation has been described in several cancers, including CRC. In addition, demethylation or overexpression of LATS1 has been shown to decrease YAP expression, resulting in increased apoptosis and inhibition of cell proliferation [34]. Similar results have been found with MST1/2, although MST1/2 appears to have less effect on YAP expression [35]. Previously, activation of LATS1/2 by MST1/2 was shown to negatively regulate the function of YAP1 by inducing phosphorylation of YAP1 on Ser 127 and Ser 358 [36], suggesting that downregulation of LATS1 and MST1/2 may elevate levels of YAP and promote a more invasive phenotype. In our study, SDC2 expression levels also influenced the expression of LATS1, MST1, and MST2, and decreased expression of these proteins was observed following SDC2 overexpression. Several studies have reported that SDC2 methylation is associated with CRC [21,37,38]. In one study, an extremely high level of aberrant SDC2 methylation was found in 97.8% of primary tumors in patients with CRC [37]. Thus, SDC2 methylation may have an important role in promoting the EMT phenotype. Further studies are required to elucidate the precise mechanisms through which SDC2 methylation regulates the YAP pathway.

Since multiple studies have implicated SDC2 in the progression of cancer through increased EMT [19], we next examined the expression of genes that are involved in the regulation of SDC2 and also participate in EMT, namely, BMP4, CTGF, and FOXM1. We

found that knockdown or overexpression of SDC2 affected BMP4, CTGF, and FOXM1 expression levels in a similar way. Moreover, silencing of YAP also led to a reduction in BMP4, CTGF, and FOXM1 expression levels. BMP4 has recently been associated with YAP-dependent regulation of EMT [39]. The progression of SMAD1-driven EMT in cancer has been found to rely on matrix rigidity and YAP through interactions with CDK8/19. Serrao et al. found that inhibiting CDK8/19 led to changes in YAP nuclear localization, as well as levels of tumor cell invasion, EMT-associated transcription factors, and E-cadherin expression [39]. YAP1 has also been found to influence the expression of CTGF in CRC [40]. Similar to our results with SDC2, FGF8 has been found to fully induce the nuclear localization of YAP1 to enhance the transcriptional expression of CTGF [40]. Likewise, we found that phosphorylated YAP localized to the nucleus where it enhanced the transcriptional activity of SDC2 and CTGF. The transcriptional activation of FOXM1 was also enhanced by nuclear localization of YAP. Our findings are consistent with previous reports in other types of cancer that found that deregulation of the Hippo pathway led to elevated YAP and FOXM1 levels and a more invasive phenotype [41]. FOXM1 is thought to directly interact with the YAP transcriptional complex [41,42].

To conclude, in the current study, we demonstrate that YAP and SDC2 are highly expressed in CRC. Silencing the expression of YAP and SDC2 resulted in a less invasive phenotype and reduced tumorigenesis. SDC2 expression influenced that the expression of LATS1, MST1, and MST2, which are components of the Hippo pathway, and have been shown to regulate the nuclear localization of YAP. Overexpression of SDC2 reversed the inhibition of EMT-related proteins caused when YAP expression is silenced. YAP and SDC2 were found to colocalize in the nucleus, and co-immunoprecipitation assays confirmed that endogenous YAP associated with SDC2. Although previous studies have examined the role of YAP or SDC2 in CRC, our study is the first to examine YAP and SDC2 in combination. Our data have highlighted the significance of the interaction between YAP and SDC2 in EMT and CRC progression, and have identified YAP and SDC2 as potential therapeutic targets for CRC. Overall, our findings have not only furthered the understanding of the complex interactions involved in the regulation of EMT by the YAP/Hippo pathways but will also be beneficial for the development of prognostic markers and more effective therapeutics against metastatic drug-resistant CRC.

Ethics approval and consent to participate

The study was approved by the Institutional Review Committee of the 989th Hospital of The Joint Logistics Support Force of PLA in accordance with the ethical standards outlined in the Declaration of Helsinki. Standard animal care and laboratory guidelines were followed according to the IACUC protocol.

Consent for publication

Written informed consent was obtained from all patients.

Availability of data and materials

Not applicable.

Author contribution statement

Yang Yang: Conceived and designed the experiments; Performed the experiments; Analyzed and interpreted the data; Contributed reagents, materials, analysis. Tools or data; Wrote the paper. Yong Li Cao: Conceived and designed the experiments; Performed the experiments; Wrote the paper. Wen Hang Wang: Conceived and designed the experiments; Performed the experiments; Analyzed and interpreted the data. Shou Sen Shi: Performed the experiments. Yuan Yao Zhang: Bing Bing Lv: Analyzed and interpreted the data. Wei Wei Yang: Ming Li: Analyzed and interpreted the data; Contributed reagents, materials, analysis tools or data.Dong Wei: Conceived and designed the experiments.

Funding statement

This work was supported by CIMF (grant number: CIMF-F-H001-301).

Data availability statement

Data will be made available on request.

Declaration of competing interest

The authors declare that they have no known competing financial interests or personal relationships that could have appeared to influence the work reported in this paper.

Acknowledgements

Not applicable.

References

[1] M. Arnold, M.S. Sierra, M. Laversanne, I. Soerjomataram, A. Jemal, F. Bray, Global patterns and trends in colorectal cancer incidence and mortality, Gut 66 (2017) 683–691.
[2] F.A. Haggar, R.P. Boushey, Colorectal cancer epidemiology: incidence, mortality, survival, and risk factors, Clin. Colon Rectal Surg. 22 (2009) 191–197.
[3] T. Armaghany, J.D. Wilson, Q. Chu, G. Mills, Genetic alterations in colorectal cancer, Gastrointest Cancer Res 5 (2012) 19–27.
[4] D.V.F. Tauriello, A. Calon, E. Lonardo, E. Batlle, Determinants of metastatic competency in colorectal cancer, Mol. Oncol. 11 (2017) 97–119.
[5] J. Massagué, A.C. Obenauf, Metastatic colonization by circulating tumour cells, Nature 529 (2016) 298–306.
[6] J. Xu, S. Lamouille, R. Derynck, TGF-B-induced epithelial to mesenchymal transition, Cell Res. 19 (2009) 156–172.
[7] R.C. Bates, B.M. Pursell, A.M. Mercurio, Epithelial-mesenchymal transition and colorectal cancer: gaining insights into tumor progression using LIM 1863 cells, Cells Tissues Organs 185 (2007) 29–39.
[8] I.A. Darby, N. Zakuan, F. Billet, A. Desmoulière, The myofibroblast, a key cell in normal and pathological tissue repair, Cell. Mol. Life Sci. 73 (2016) 1145–1157.
[9] C. Mehner, D.C. Radisky, Triggering the landslide: the tumor-promotional effects of myofibroblasts, Exp. Cell Res. 319 (2013) 1657–1662.
[10] T. Vu, P. Datta, Regulation of EMT in colorectal cancer: a culprit in metastasis, Cancers 9 (2017) 171.
[11] S.H.S. Lim, T.M. Becker, W. Chua, W.L. Ng, P. De Souza, K.J. Spring, Circulating tumour cells and the epithelial mesenchymal transition in colorectal cancer, J. Clin. Pathol. 67 (2014) 848–853.
[12] C.-L. Kim, S.-H. Choi, J.-S. Mo, Role of the Hippo pathway in fibrosis and cancer, Cells 8 (2019) 468.
[13] H. Zeng, A. Ortiz, P.-F. Shen, C.-J. Cheng, Y.-C. Lee, G. Yu, et al., Angiomotin regulates prostate cancer cell proliferation by signaling through the Hippo-YAP pathway, Oncotarget 8 (2017) 10145–10160.
[14] Z. Jiang, C. Zhou, L. Cheng, B. Yan, K. Chen, X. Chen, et al., Inhibiting YAP expression suppresses pancreatic cancer progression by disrupting tumor-stromal interactions, J. Exp. Clin. Cancer Res. 37 (2018) 69.
[15] D. Pan, The hippo signaling pathway in development and cancer, Dev. Cell 19 (2010) 491–505.
[16] B. Zhao, L. Li, L. Wang, C.Y. Wang, J. Yu, K.L. Guan, Cell detachment activates the Hippo pathway via cytoskeleton reorganization to induce anoikis, Genes Dev. 26 (2012) 54–68.
[17] E.H.Y. Chan, M. Nousiainen, R.B. Chalamalasetty, A. Schäfer, E.A. Nigg, H.H.W. Sillje, The Ste20-like kinase Mst2 activates the human large tumor suppressor kinase Lats1, Oncogene 24 (2005) 2076–2086.
[18] G. David, X.M. Bai, B. Van der Schueren, P. Marynen, J.J. Cassiman, H. Van den Berghe, Spatial and temporal changes in the expression of fibroglycan (syndecan-2) during mouse embryonic development, Development 119 (1993) 841–854.
[19] M. Mytilinaiou, D. Nikitovic, A. Berdiaki, A. Kostouras, A. Papoutsidakis, A.M. Tsatsakis, et al., Emerging roles of syndecan 2 in epithelial and mesenchymal cancer progression, IUBMB Life 69 (2017) 824–833.
[20] R. Hua, J. Yu, X. Yan, Q. Ni, X. Zhi, X. Li, et al., Syndecan-2 in colorectal cancer plays oncogenic role via epithelial-mesenchymal transition and MAPK pathway, Biomed. Pharmacother. (2020) 121.
[21] B.K. Barták, A. Kalmár, B. Péterfia, V. Patai Á, O. Galamb, G. Valcz, et al., Colorectal adenoma and cancer detection based on altered methylation pattern of SFRP1, SFRP2, SDC2, and PRIMA1 in plasma samples, Epigenetics 12 (2017) 751–763.
[22] J. Chen, H. Sun, W. Tang, L. Zhou, X. Xie, Z. Qu, et al., DNA methylation biomarkers in stool for early screening of colorectal cancer, J. Cancer 10 (2019) 5264–5271.
[23] J. Ning, Y. Zhao, Y. Ye, J. Yu, Opposing roles and potential antagonistic mechanism between TGF-β and BMP pathways: implications for cancer progression, EBioMedicine 41 (2019) 702–710.
[24] S. Braig, S. Wallner, B. Junglas, R. Fuchshofer, A.-K. Bosserhoff, CTGF is overexpressed in malignant melanoma and promotes cell invasion and migration, Br. J. Cancer 105 (2011) 231–238.
[25] K. Yang, B. Jiang, Y. Lu, Q. Shu, P. Zhai, Q. Zhi, et al., FOXM1 promotes the growth and metastasis of colorectal cancer via activation of β-catenin signaling pathway, Cancer Manag. Res. 11 (2019) 3779–3790.
[26] R.C. Bates, A.M. Mercurio, The epithelial-mesenchymal transition (EMT) and colorectal cancer progression, Cancer Biol. Ther. 4 (2005) 365–370.
[27] A.K. Roseweir, C.Y. Kong, J.H. Park, L. Bennett, A.G.M.T. Powell, J. Quinn, et al., A novel tumor-based epithelial-to-mesenchymal transition score that associates with prognosis and metastasis in patients with Stage II/III colorectal cancer, Int. J. Cancer 144 (2019) 150–159.
[28] Y. Zhou, Y. Wang, W. Zhou, T. Chen, Q. Wu, V.K. Chutturghoon, et al., YAP promotes multi-drug resistance and inhibits autophagy-related cell death in hepatocellular carcinoma via the RAC1-ROS-mTOR pathway, Cancer Cell Int. 19 (2019).
[29] C.D.K. Nguyen, C. Yi, YAP/TAZ signaling and resistance to cancer therapy, Trends in Cancer 5 (2019) 283–296.
[30] R. Song, D. Gu, L. Zhang, X. Zhang, B. Yu, B. Liu, et al., Functional significance of Hippo/YAP signaling for drug resistance in colorectal cancer, Mol. Carcinog. 57 (2018) 1608–1615.
[31] P. Vandenberghe, M. Delvaux, P. Hagué, C. Erneux, J.M. Vanderwinden, Potentiation of imatinib by cilostazol in sensitive and resistant gastrointestinal stromal tumor cell lines involves YAP inhibition, Oncotarget 10 (2019) 1798–1811.
[32] X. Wang, B. Wu, Z. Zhong, Downregulation of YAP inhibits proliferation, invasion and increases cisplatin sensitivity in human hepatocellular carcinoma cells, Oncol. Lett. 16 (2018) 585–593.
[33] T. Moroishi, H.W. Park, B. Qin, Q. Chen, Z. Meng, S.W. Plouffe, et al., A YAP/TAZ-induced feedback mechanism regulates Hippo pathway homeostasis, Genes Dev. 29 (2015) 1271–1284.
[34] K.H. Chen, J. He, D.L. Wang, J.J. Cao, M.C. Li, X.M. Zhao, et al., Methylation-associated inactivation of LATS1 and its effect on demethylation or overexpression on YAP and cell biological function in human renal cell carcinoma, Int. J. Oncol. 45 (2014) 2511–2521.
[35] Y. Ma, Y. Yang, F. Wang, Q. Wei, H. Qin, Hippo-YAP signaling pathway: a new paradigm for cancer therapy, Int. J. Cancer 137 (2015) 2275–2286.
[36] T. Shimomura, N. Miyamura, S. Hata, R. Miura, J. Hirayama, H. Nishina, The PDZ-binding motif of Yes-associated protein is required for its co-activation of TEAD-mediated CTGF transcription and oncogenic cell transforming activity, Biochem. Biophys. Res. Commun. 443 (2014) 917–923.
[37] T. Oh, N. Kim, Y. Moon, M.S. Kim, B.D. Hoehn, C.H. Park, et al., Genome-wide identification and validation of a novel methylation biomarker, SDC2, for blood-based detection of colorectal cancer, J Mol Diagnostics 15 (2013) 498–507.
[38] B. Molnár, O. Galamb, B. Péterfia, B. Wichmann, I. Csabai, A. Bodor, et al., Gene promoter and exon DNA methylation changes in colon cancer development - mRNA expression and tumor mutation alterations, BMC Cancer 18 (2018).
[39] A. Serrao, L.M. Jenkins, A.A. Chumanevich, B. Horst, J. Liang, M.L. Gatza, et al., Mediator kinase CDK8/CDK19 drives YAP1-dependent BMP4-induced EMT in cancer, Oncogene 37 (2018) 4792–4808.
[40] R. Liu, S. Huang, Y. Lei, T. Zhang, K. Wang, B. Liu, et al., FGF8 promotes colorectal cancer growth and metastasis by activating YAP1, Oncotarget 6 (2015) 935–952.
[41] T.S.K. Eisinger-Mathason, V. Mucaj, K.M. Biju, M.S. Nakazawa, M. Gohil, T.P. Cash, et al., Deregulation of the Hippo pathway in soft-tissue sarcoma promotes FOXM1 expression and tumorigenesis, Proc. Natl. Acad. Sci. U.S.A. 112 (2015) E3402–E3411.
[42] Q. Fan, Q. Cai, Y. Xu, FOXM1 is a downstream target of LPA and YAP oncogenic signaling pathways in high grade serous ovarian cancer, Oncotarget 6 (2015) 27688–27699.